Hysteresis, reentrance, and glassy dynamics in systems of self-propelled rods

Hui-Shun Kuan[a], Robert Blackwell[b], Loren E. Hough[b], Matthew A. Glaser[b], and M. D. Betterton[b]
[a] *Department of Chemistry and Biochemistry, University of Colorado at Boulder, Boulder, CO 80302, USA*
[b] *Department of Physics, University of Colorado at Boulder, Boulder, CO 80302, USA*
(Dated: September 28, 2015)

Non-equilibrium active matter made up of self-driven particles with short-range repulsive interactions is a useful minimal system to study active matter as the system exhibits collective motion and nonequilibrium order-disorder transitions. We studied high-aspect-ratio self-propelled rods over a wide range of packing fraction and driving to determine the nonequilibrium state diagram and dynamic properties. Flocking and nematic-laning states occupy much of the parameter space. In the flocking state the average internal pressure is high and structural and mechanical relaxation times are long, suggesting that rods in flocks are in a translating glassy state despite overall flock motion. In contrast, the nematic-laning state shows fluid-like behavior. The flocking state occupies regions of the state diagram at both low and high packing fraction separated by nematic-laning at low driving and a history-dependent region at higher driving; the nematic-laning state transitions to the flocking state for both compression and expansion. We propose that the laning-flocking transitions are a type of glass transition which, in contrast to other glass-forming systems, can show fluidization as density increases. The fluid internal dynamics and ballistic transport of the nematic-laning state may promote collective dynamics of rod-shaped microorganisms.

PACS numbers: 87.10.Tf,64.60.Cn,05.65.+b

arXiv:1407.4842v2 [cond-mat.soft] 25 Sep 2015

Active matter made up of self-driven particles exhibits novel physical properties include collective motion, nonequilibrium order-disorder transitions, and anomalous fluctuations and mechanical response[1]. Understanding active matter may aid the development of new technologies including autonomously motile and self-healing synthetic materials. Examples of active matter include animal flocks[2], crawling and swimming cells[3–5], vibrated granular materials[6,7], self-propelled colloidal particles[8,9], and the cellular cytoskeleton and cytoskeletal extracts[10].

Among active matter, self-propelled rods (SPR) provide a useful minimal model system. Self-propulsion and excluded volume interactions via a short-range repulsive potential are the only ingredients; rod alignment occurs through collisions. Experiments which may be approximated as SPR include vibrated granular rods[11], motion of cytoskeletal filaments on a motor-bound surface[10,12], and surface or film swarming of rod-like bacteria[4,5,13,14]. Because of their simplicity SPR are attractive to simulation study[14–21] and have also been the focus of analytic theory[19,22]. SPR display a rich variety of dynamic states, including collective motion[7,23–28] and formation of dynamic clusters[12,16,17,20,21,28,29].

For SPR, rod shape, density, and driving are important in determining the dynamic behavior[14,16–22]. For low driving, equilibrium-like isotropic and nematic liquid crystal phases are recovered[21,22]. For higher driving, dynamic states characterized by the appearance of flocks, stripes, and swirls appear[14,16,19–22]. Baskaran and Marchetti derived a hydrodynamic model from the kinetics of SPR with two-rod collisions and determined a state diagram from linear stability analysis of homogeneous states, finding that activity lowers the isotropic-nematic transition density[22]. Previous simulation work has observed flocking and laning states similar to those we study here[19–21], but did not measure on dynamic state transitions, hysteresis, or structural and mechanical properties. In this work, by studying the state diagram over a broader range of parameters with extensive expansion and compression simulations and mechanical and structural characterization, we demonstrate strong hysteresis, the emergence of glassy dynamics in the flocking state, and reentrant fluidization.

We studied self-propelled 2D spherocylinders with Brownian dynamics, as in previous work[20], using the computational scheme of Tao et al.[30] developed for equilibrium simulations of concentrated solutions of high-aspect-ratio particles. Rods have length L and diameter σ. The center-of-mass and orientational equations of motion for rod i with center-of-mass position $\mathbf{r}_i$ and orientation $\mathbf{u}_i$ are

$$\mathbf{r}_i(t+\delta t) = \mathbf{r}_i(t) + \mathbf{\Gamma}_i^{-1}(t)\cdot\mathbf{F}_i(t)\delta t + \delta\mathbf{r}_i(t), \quad (1)$$

$$\mathbf{u}_i(t+\delta t) = \mathbf{u}_i(t) + \frac{1}{\gamma_r}\mathbf{T}_i(t)\times\mathbf{u}_i(t)\delta t + \delta\mathbf{u}_i(t), \quad (2)$$

where the random displacements $\delta\mathbf{r}_i(t)$ and $\delta\mathbf{u}_i(t)$ are Gaussian-distributed, $\mathbf{\Gamma}_i^{-1}(t)$ is the inverse friction tensor, γ_r is the rotational drag coefficient, and $\mathbf{F}_i(t)$ and $\mathbf{T}_i(t)$ are the the deterministic force and torque on particle i[31]. Excluded-volume interactions between particles are modeled by the WCA potential as a function of the minimum distance s_{ij} between the two finite line segments of length L that define the axes of particles i and j[31,32]. The self-propulsion force is directed along the particle axis with $\mathbf{F}_i^{\mathrm{drive}} = F_D\mathbf{u}_i$. In the absence of nonequibrium driving, this model has been well-characterized both in 2D[33] and 3D[34].

We nondimensionalize using the length σ, energy k_BT, and time $\tau = D/\sigma^2$, where D is the diffusion coefficient of a sphere of diameter σ. The three dimensionless parameters are the rod aspect ratio $R = L/\sigma$, fixed at 40, the

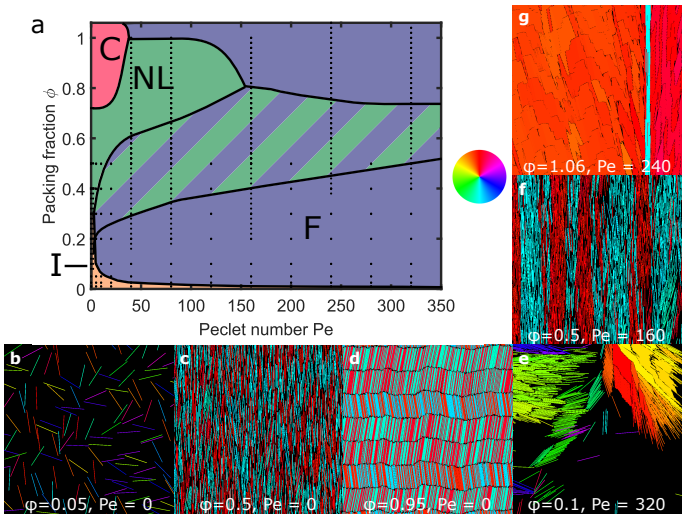

FIG. 1. Nonequilibrium state diagram and snapshots of self-propelled rods of aspect ratio 40. (a) State diagram as a function of Peclet number and packing fraction. Points indicate parameter sets of simulations. Solid lines indicate boundaries of regions of stability of different initial conditions. I (orange), isotropic state; F (purple) flocking state; NL (green) nematic-laning state; C (pink) crystalline state. Green-purple striping indicates region where both flocking and nematic-laning initial conditions are stable. (b-g) Simulation snapshots at indicated packing fraction and Peclet number. Rods are colored by orientation according to the colorwheel. (b) Isotropic. (c) Nematic. (d) Crystal. (e) Flocking. (f) Nematic–laning. (g) Flocking.

packing fraction $\phi = A_{\rm rods}/A_{\rm system}$, and the translational Peclet number $\mathrm{Pe} = F_D L/(k_B T)$. We varied ϕ between 0.01 and 1.04 (where $\phi > 1$ is possible due to the slight softness of the repulsive potential), and Pe between 0 and 320. We simulated $N = 4000$ rods in a square, periodic box. Most simulations were initialized in an equilibrium isotropic, nematic, or crystalline initial condition, then nonequilibrium activity was turned on and the system was allowed to run for $10^7\tau$. The simulation measurement run was $10^7\tau$, and the time step $\Delta t = 0.25\tau$.

At zero or low driving, we find equilibrium isotropic, nematic, and crystalline states (fig. 1a-d). While we did not map the equilibrium phase transitions in detail, our observations are consistent with previous work[33]. As the Peclet number increases, lower packing fractions roughly corresponding to the equilibrium isotropic phase typically show flocking behavior characterized by collective motion of clusters of various sizes coexisting with a low-density vapor (fig. 1e), as observed previously[16,17,20,28,29]. While the flocking state remains globally isotropic (consistent with previous predictions[22]), the formation of dense aligned clusters is characterized by short-range density correlations that lead to peaks in the pair distribution function and the emergence of polar and nematic orientational correlations that persist over a cluster-size length scale (fig. S1, and other data not shown). Rod mean-squared displacements are ballistic at short times, turning over to diffusive at long times due to flock reorientation. The long-time angular mean-squared displacement is diffusive.

The flocking state shows large density heterogeneity suggestive of two-phase coexistence between dense orientationally ordered clusters and low-density isotropic rods. In previous work on self-propelled spheres or disks, two-phase coexistence of a dense cluster and a dilute vapor was observed that appears qualitatively similar to what we observe here[9,35–37]. However, flocks are dynamic and are constantly merging, breaking up, and exchanging particles with the dilute region[16,29]. We identified flocks based on measurements of the contact number $c_i = \sum_{i\neq j} e^{-s_{ij}^2}$ and local polar order parameter $p_i = \sum_{i\neq j} \mathbf{u}_i \cdot \mathbf{u}_j e^{-s_{ij}^2}/c_i$ of rod i. Two-dimensional histograms show peaks in the density for large p_i over a range of c_i (fig. S2); individual flocks were defined as collections of neighboring flock particles[31] (fig. S2). We identified flocks and isolated them in a box empty of other rods; this led the isolated flock to break up, demonstrating that flocks are not stable as isolated clusters. Flock size distributions are stable in time and power law in form with an exponential cutoff, as observed previously[4,16,29,38,39] (fig. S3).

As the Peclet number increases, higher packing fractions driven from an equilibrium nematic or crystal typically show nematic-laning behavior characterized by the formation of polar lanes of upward- and downward-moving particles (fig. 1f,g). The density is approximately uniform and the orientational order is globally nematic in most cases with polar correlations on the scale of the system size in the alignment direction and on the scale of a typical lane width perpendicular to the alignment direction (fig. S1 and data not shown). Rod mean-squared displacements are ballistic in the alignment direction and diffusive perpendicular, while the angular mean-squared displacement is bounded due to the the maximum angular deviation of rods. The emergence of lanes in SPR and related models has been observed in previous simulation studies[14,19–21,40], and laning has been studied previously for spherical particles both in experiments[41] and theory/simulation[42,43]. Laning occurs because of the differences in collisions experienced by rods as a function of their polar environment: a rod moving surrounded by opposite polarity rods will experience more collisions, and therefore more momentum transfer, than when surrounded by rods of similar polarity. A rod surrounded by others of similar polarity will therefore experience reduced lateral movement and be less likely to leave the polar lane[20,42].

To characterize the transitions between nematic-laning and flocking states, we performed expansion and compression runs in which the packing fraction was changed by $\Delta\phi = 0.02$, the simulation was run for $10^7\tau$ to reach a dynamic steady state, and then measurements were performed over an additional $10^7\tau$. The appearance of the nematic-laning state is dependent on initial conditions; lanes with equal numbers of up- and down-moving

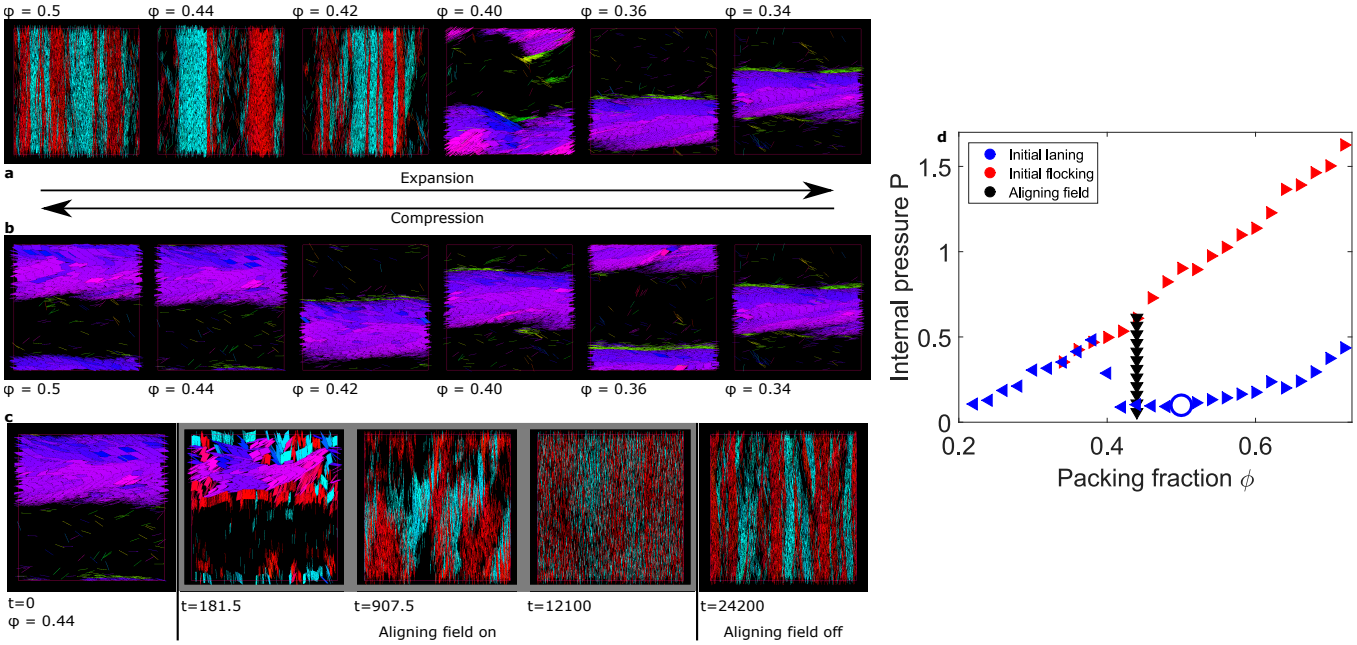

FIG. 2. Hysteresis in simulations under expansion, compression, and with an applied field. (a) Simulation snapshots of an expansion run initially in the nematic-laning state at $\phi = 0.5$ (far left). When the packing fraction reaches 0.4 the system transitions to the flocking state. (b) Simulation snapshots of a compression run initially in the flocking state at $\phi = 0.34$ (far right). The system remains in the flocking state when compressed. (c) Simulation snapshots of run with applied nematic aligning field beginning in the flocking state at $\phi = 0.44$ (far left). The applied field breaks up the flock and allows a return to the nematic-laning state after the field is removed (far right). (d) Internal pressure for systems shown in (a-c). Blue, initial nematic-laning state as shown in (a); red initial flocking state as shown in (b); black, system with nematic aligning field as shown in (c).

rods result from initialization with an equilibrium nematic state and the high rod packing fraction which prevents rod reorientation. Upon expansion, the system undergoes an abrupt transition to the flocking state (fig. 2a), while compression simulations subsequently started in the flocking typically remain in the flocking state (fig. 2b). If we apply a nematic aligning field to a compressed flocking state, the induced rod reorientation can break up the flock and allow a transition back to the nematic-laning state (fig. 2c). This strong hysteresis is another signature of an abrupt dynamic transition between the laning and flocking states. While previous work has examined the nonequilibrium state diagram of SPR[14,16,19–22], to our knowledge this is the first study to demonstrate strong hysteresis in this system.

McCandlish et al. found the laning state to be unstable to break up[20]. While the strong hysteresis we observe makes it difficult to guarantee that any nonequilibrum state is stable for infinite time, our expansion and compression simulations effectively extended our simulation times up to $2\times10^8\tau$ in the nematic-laning state, and upon reaching the transition boundary we typically see break up of the lanes into flocks within the $10^7\tau$ equilibration run. Therefore in our system the laning phase appears to be stable, consistent with other work[14,19,21]. The instablity observed by McCandlish et al. may be related to the reentrance we observe if the simulations were performed near the upper limit of stability of the nematic-laning state.

During expansion runs, the isotropic internal pressure P_o, measured by the virial[31], abruptly changes by a factor of 2–10 at the transitions between nematic-laning and flocking states (fig. 2d). (The nature of the pressure in active systems has been the subject of recent work[44]; here we consider the internal pressure determined by the virial only.) At the highest packing fractions the internal pressure approaches a plateau value near 10 for all systems, suggesting that a pure dense flocking state has been reached. The internal pressure of the flocking state lies along an envelope that decreases with decreasing packing fraction as the rod flocking/isotropic fraction varies. Nematic-laning systems undergo transitions to flocking upon both expansion and compression (fig. 3a,b, open circles labeled by arrows indicate starting simulations of expansion/compression runs). Flocking systems, typically remain flocking upon compression, but for low packing fractions a transition back to the nematic-laning state upon compression can occur (fig. 3b, open circles labeled by downward-pointing arrows indicate starting simulations of compression runs).

The dense clusters and high pressure in the flocking state suggest that the clusters may have slow internal dynamics. To characterize structural relaxation we measured the normalized structure-factor autocorrelation

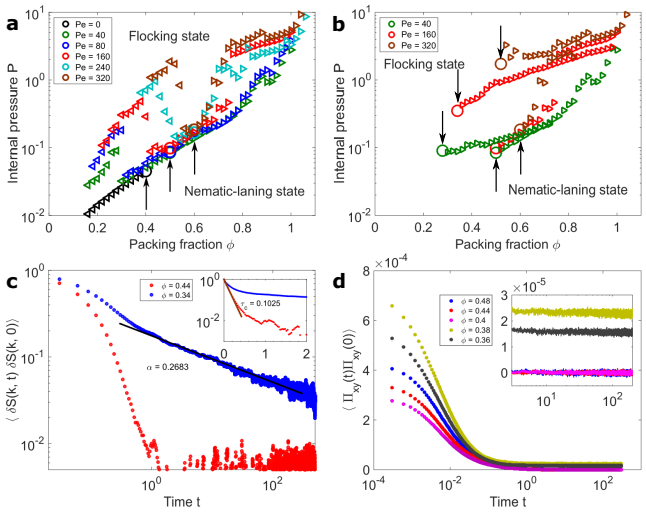

FIG. 3. Mechanical and structural properties of the nematic-laning and flocking states. (a,b) Internal pressure as a function of packing fraction during expansion (left-handed triangles) and compression (right-handed triangles) runs for simulations with varying Peclet number. The black arrows and open circles indicate the initial state of each run. (c) Structure-factor autocorrelation as a function of time for Pe=160 and systems in the laning ($\phi = 0.44$, red) and flocking ($\phi = 0.34$, blue) states for the peak nearest wave number $k = 2\pi/\sigma$. The autocorrelation exhibits exponential decay in the nematic-laning state with characteristic time $\tau_c = 0.10$ and power-law decay in the flocking state with the exponent $\alpha = 0.27$ as indicated. Inset, semi-log plot. (d) Stress-tensor autocorrelation as a function of time for Pe=160 and systems in the nematic-laning ($\phi = 0.4 - 0.48$) and flocking ($\phi = 0.36 - 0.38$) states. Inset, zoomed view of long-time tail.

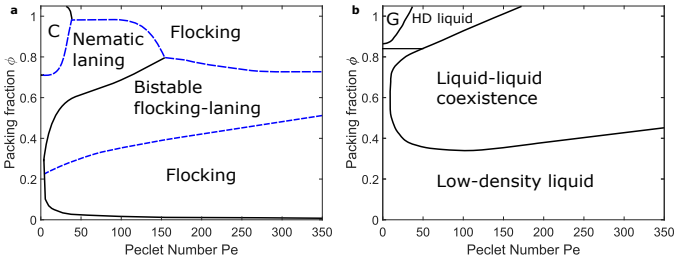

FIG. 4. Comparison of self-propelled rod and sphere nonequilibrium state diagrams. (a) SPR state diagram from this study as a function of the translational Peclet number. Blue dashed lines show limits of stability of the nematic-laning state characterized by ballistic transport along the lane. (b) Self-propelled sphere state diagram as a function of the rotational Peclet number, adapted from Fily, Henkes, and Marchetti[37].

function $C(t)/C(0)$, where $C(t) = \langle \delta S(k,t)\delta S(k,0)\rangle$, k is the magnitude of the wavevector and $\delta S(k,t) = S(k,t) - \langle S(k,t)\rangle$ is the fluctuation in the the angle-averaged structure factor $S(k,t) = \frac{1}{2\pi N}\int_0^{2\pi} d\phi \rho(\mathbf{k},t)\rho(-\mathbf{k},t)$[31]. Because the angle-averaged structure factor is rotationally invariant, its autocorrelation probes internal structural relaxation of flocks and lanes but is insensitive to flock reorientation. We determined the location of the peak nearest to wave number $k = 2\pi/\sigma$, corresponding to side-by-side filaments separated by approximately one diameter. In the nematic-laning state, the structure-factor autocorrelation exponentially decays (fig. 3c, red curve). However in the flocking state, the structure-factor autocorrelation has a power-law tail, indicating slow structural relaxation (fig. 3c, blue curve). Expansion to lower packing fractions has little effect on the power-law exponent, indicating that slow relaxation of dense clusters controls the decay of the structure-factor autocorrelation. Compression leads to a density-dependent exponent (fig. S4).

Mechanical relaxation was measured by the autocorrelation function of the off-diagonal internal stress tensor $\langle \Pi_{xy}(t)\Pi_{xy}(0)\rangle$[31]. In the nematic-laning state, the stress autocorrelation drops to zero around $t = 1$ (fig. 3d, blue, red, and purple curves). In the flocking state, the stress autocorrelation function relaxes to a small but long-lived plateau (fig. 3d, yellow-green and grey curves). Consistent with this, the effective shear viscosity measured via the Green-Kubo relation[31] shows a factor of 10^3 increase upon transition from the nematic-laning to the flocking state for Pe=80 (fig. S4).

The large increases in pressure and shear viscosity and slowed structural and mechanical relaxation that occurs upon transition from nematic-laning to flocking suggest that this is a type of glass transition in which flocks, although collectively moving, have an internally glassy, solid-like structure. Related observations were made in an experimental system with self-propelled colloids, for which nonequilibrium driving promoted formation of small, mobile crystalline clusters[9]. Related phase separation between a low-density gas and high-density liquid, glassy clusters or crystals has been observed both in experiments[9,35] and theory and simulations[36,37]. In contrast to both recent active jamming work and classic granular jamming[45], in our self-propelled rod system the increased importance of aligning interactions means that the transition to the translating glassy flocking state can occurs both as density is raised and *lowered*. This reentrant fluidization appears to be a novel feature of this transition in systems of self-propelled rods.

Self-propelled rods couple shape anisotropy to directional polarity, in contrast to self-propelled spheres. This enables a rich state diagram for SPR with important implications for transport (fig. 4). Orientational ordering allows SPR to form a nematic-laning state at high packing fraction characterized by fluid internal dynamics and ballistic transport along the lanes. Much of the same region of parameter space of self-propelled spheres consists of phase-separated liquid-liquid coexistence (fig. 4)[36,37] for which particle dynamics are diffusive[37] and the formation of dense clusters limits particle motion. Perhaps the physics of laning is important for collective motion of rod-shaped microorganisms such as *Myxococcus*

xanthus, which during fruiting-body formation assemble into dense streams qualitatively similar to the lanes we observe[5]. Ballistic transport through coupling of orientational order and self propulsion may give an advantage to rod-shaped rather than spherical bacteria.

ACKNOWLEDGMENTS

We thank Lisa Manning, John Toner, Leo Radzihovsky, and Joel Eaves for useful discussions. This work was supported by NSF grants MRSEC-DMR-0820579, EF-ATB-1137822, and DMR-0847685 and NIH grant T32 GM-065103. This work utilized the Janus supercomputer, which is supported by the National Science Foundation (CNS-0821794) and the University of Colorado Boulder. The Janus supercomputer is a joint effort of the University of Colorado Boulder, the University of Colorado Denver and the National Center for Atmospheric Research. Janus is operated by the University of Colorado Boulder.

[1] S. Ramaswamy, Annual Review of Condensed Matter Physics **1**, 323 (2010); M. C. Marchetti, J. F. Joanny, S. Ramaswamy, T. B. Liverpool, J. Prost, M. Rao, and R. A. Simha, Reviews of Modern Physics **85**, 1143 (2013).
[2] A. Cavagna, A. Cimarelli, I. Giardina, G. Parisi, R. Santagati, F. Stefanini, and M. Viale, Proceedings of the National Academy of Sciences **107**, 11865 (2010).
[3] W.-J. Rappel, A. Nicol, A. Sarkissian, H. Levine, and W. F. Loomis, Physical Review Letters **83**, 1247 (1999); L. H. Cisneros, J. O. Kessler, S. Ganguly, and R. E. Goldstein, Physical Review E **83**, 061907 (2011).
[4] H. P. Zhang, A. Be'er, E.-L. Florin, and H. L. Swinney, Proceedings of the National Academy of Sciences **107**, 13626 (2010).
[5] S. Thutupalli, M. Sun, F. Bunyak, K. Palaniappan, and J. W. Shaevitz, arXiv:1410.7230 [physics, q-bio] (2014).
[6] V. Narayan, S. Ramaswamy, and N. Menon, Science **317**, 105 (2007).
[7] J. Deseigne, O. Dauchot, and H. Chaté, Physical Review Letters **105** (2010), 10.1103/PhysRevLett.105.098001.
[8] A. Bricard, J.-B. Caussin, N. Desreumaux, O. Dauchot, and D. Bartolo, Nature **503**, 95 (2013).
[9] J. Palacci, S. Sacanna, A. P. Steinberg, D. J. Pine, and P. M. Chaikin, Science **339**, 936 (2013).
[10] F. Nedelec, T. Surrey, A. C. Maggs, and S. Leibler, Nature **389**, 305 (1997); T. Butt, T. Mufti, A. Humayun, P. B. Rosenthal, S. Khan, S. Khan, and J. E. Molloy, Journal of Biological Chemistry **285**, 4964 (2010).
[11] A. Kudrolli, G. Lumay, D. Volfson, and L. S. Tsimring, Physical Review Letters **100**, 058001 (2008).
[12] V. Schaller, C. Weber, C. Semmrich, E. Frey, and A. R. Bausch, Nature **467**, 73 (2010).
[13] A. Sokolov, I. S. Aranson, J. O. Kessler, and R. E. Goldstein, Physical Review Letters **98**, 158102 (2007).
[14] H. H. Wensink, J. Dunkel, S. Heidenreich, K. Drescher, R. E. Goldstein, H. Löwen, and J. M. Yeomans, Proceedings of the National Academy of Sciences **109**, 14308 (2012).
[15] P. Kraikivski, R. Lipowsky, and J. Kierfeld, Physical Review Letters **96** (2006), 10.1103/PhysRevLett.96.258103.
[16] F. Peruani, A. Deutsch, and M. Bär, Physical Review E **74** (2006), 10.1103/PhysRevE.74.030904.
[17] Y. Yang, V. Marceau, and G. Gompper, Physical Review E **82**, 031904 (2010).
[18] F. Peruani, T. Klauss, A. Deutsch, and A. Voss-Boehme, Physical Review Letters **106**, 128101 (2011).
[19] H. H. Wensink and H. Löwen, Journal of Physics: Condensed Matter **24**, 464130 (2012).
[20] S. R. McCandlish, A. Baskaran, and M. F. Hagan, Soft Matter **8**, 2527 (2012).
[21] M. Abkenar, K. Marx, T. Auth, and G. Gompper, Physical Review E **88**, 062314 (2013).
[22] A. Baskaran and M. C. Marchetti, Physical Review Letters **101**, 268101 (2008); Physical Review E **77** (2008), 10.1103/PhysRevE.77.011920.
[23] T. Vicsek, A. Czirók, E. Ben-Jacob, I. Cohen, and O. Shochet, Physical Review Letters **75**, 1226 (1995); G. Grégoire and H. Chaté, Physical Review Letters **92**, 025702 (2004); H. Chaté, F. Ginelli, and F. Raynaud, Physical Review E **77** (2008), 10.1103/PhysRevE.77.046113; E. Bertin, M. Droz, and G. Grégoire, Physical Review E **74** (2006), 10.1103/PhysRevE.74.022101; Journal of Physics A: Mathematical and Theoretical **42**, 445001 (2009); F. Ginelli, F. Peruani, M. Bär, and H. Chaté, Physical Review Letters **104** (2010), 10.1103/PhysRevLett.104.184502; F. Peruani, J. Starruß, V. Jakovljevic, L. Søgaard-Andersen, A. Deutsch, and M. Bär, Physical Review Letters **108**, 098102 (2012); M. Aldana, V. Dossetti, C. Huepe, V. M. Kenkre, and H. Larralde, Physical Review Letters **98**, 095702 (2007); T. Ihle, Physical Review E **88**, 040303 (2013).
[24] J. Toner and Y. Tu, Physical Review Letters **75**, 4326 (1995).
[25] S. Mishra, A. Baskaran, and M. Marchetti, Physical Review E **81** (2010), 10.1103/PhysRevE.81.061916.
[26] A. Gopinath, M. F. Hagan, M. C. Marchetti, and A. Baskaran, Physical Review E **85**, 061903 (2012).
[27] A. Peshkov, I. S. Aranson, E. Bertin, H. Chaté, and F. Ginelli, Physical Review Letters **109**, 268701 (2012).
[28] C. A. Weber, F. Thüroff, and E. Frey, New Journal of Physics **15**, 045014 (2013).
[29] F. Peruani, L. Schimansky-Geier, and M. Bär, The European Physical Journal Special Topics **191**, 173 (2011); F. Peruani and M. Bär, New Journal of Physics **15**, 065009 (2013).
[30] Y.-G. Tao, W. K. den Otter, J. T. Padding, J. K. G. Dhont, and W. J. Briels, The Journal of Chemical Physics **122**,

244903 (2005).
[31] See Supplemental Material at [URL] for details of simulation method and analysis.
[32] J. D. Weeks, D. Chandler, and H. C. Andersen, The Journal of Chemical Physics **54**, 5237 (1971).
[33] M. A. Bates and D. Frenkel, The Journal of Chemical Physics **112**, 10034 (2000).
[34] P. Bolhuis and D. Frenkel, Journal of Chemical Physics **106**, 666 (1997); S. C. McGrother, D. C. Williamson, and G. Jackson, The Journal of Chemical Physics **104**, 6755 (1996).
[35] I. Theurkauff, C. Cottin-Bizonne, J. Palacci, C. Ybert, and L. Bocquet, Physical Review Letters **108**, 268303 (2012); I. Buttinoni, J. Bialké, F. Kümmel, H. Löwen, C. Bechinger, and T. Speck, Physical Review Letters **110**, 238301 (2013).
[36] S. Henkes, Y. Fily, and M. C. Marchetti, Physical Review E **84** (2011), 10.1103/PhysRevE.84.040301; Y. Fily and M. C. Marchetti, Physical Review Letters **108**, 235702 (2012); G. S. Redner, M. F. Hagan, and A. Baskaran, Physical Review Letters **110** (2013), 10.1103/PhysRevLett.110.055701; T. Speck, J. Bialké, A. M. Menzel, and H. Löwen, Physical Review Letters **112**, 218304 (2014); H. H. Wensink, V. Kantsler, R. E. Goldstein, and J. Dunkel, Physical Review E **89**, 010302 (2014); X. Yang, M. L. Manning, and M. C. Marchetti, Soft Matter **10**, 6477 (2014); S. C. Takatori and J. F. Brady, Physical Review E **91**, 032117 (2015).
[37] Y. Fily, A. Baskaran, and M. F. Hagan, arXiv:1402.5583 [cond-mat] (2014).
[38] F. Peruani, F. Ginelli, M. Bär, and H. Chaté, in *Journal of Physics: Conference Series*, Vol. 297 (2011) p. 012014.
[39] C. J. Chen, K. Porche, I. Rayment, and S. P. Gilbert, Journal of Biological Chemistry **287**, 36673 (2012).
[40] K. H. Nagai, Y. Sumino, R. Montagne, I. S. Aranson, and H. Chaté, Physical Review Letters **114**, 168001 (2015).
[41] M. E. Leunissen, C. G. Christova, A.-P. Hynninen, C. P. Royall, A. I. Campbell, A. Imhof, M. Dijkstra, R. van Roij, and A. van Blaaderen, Nature **437**, 235 (2005); K. R. Sutterlin, A. Wysocki, A. V. Ivlev, C. Räth, H. M. Thomas, M. Rubin-Zuzic, W. J. Goedheer, V. E. Fortov, A. M. Lipaev, V. I. Molotkov, O. F. Petrov, G. E. Morfill, and H. Löwen, Physical Review Letters **102**, 085003 (2009); T. Vissers, A. Wysocki, M. Rex, H. Löwen, C. P. Royall, A. Imhof, and A. van Blaaderen, Soft Matter **7**, 2352 (2011).
[42] J. Chakrabarti, J. Dzubiella, and H. Löwen, EPL (Europhysics Letters) **61**, 415 (2003).
[43] J. Dzubiella, G. P. Hoffmann, and H. Löwen, Physical Review E **65**, 021402 (2002); R. R. Netz, EPL (Europhysics Letters) **63**, 616 (2003); J. Delhommelle, Physical Review E **71**, 016705 (2005); T. Glanz and H. Löwen, Journal of Physics: Condensed Matter **24**, 464114 (2012).
[44] A. P. Solon, J. Stenhammar, R. Wittkowski, M. Kardar, Y. Kafri, M. E. Cates, and J. Tailleur, arXiv:1412.5475 [cond-mat] (2014); A. P. Solon, Y. Fily, A. Baskaran, M. E. Cates, Y. Kafri, M. Kardar, and J. Tailleur, arXiv:1412.3952 [cond-mat] (2014); S. Takatori, W. Yan, and J. Brady, Physical Review Letters **113**, 028103 (2014).
[45] A. J. Liu and S. R. Nagel, Nature **396**, 21 (1998); C. Reichhardt and C. J. O. Reichhardt, Soft Matter **10**, 2932 (2014).